JOURNAL OF MATERIALS SCIENCE 26 (1991) 3362–3365

Deformation-mechanism map for Ti–6 wt% Al alloy

K. JANGHORBAN, S. ESMAEILI
Department of Materials Science and Engineering, Shiraz University, Shiraz, Iran

A micro-computer program was developed to plot deformation mechanism maps for metals and substitutional solid solutions such as Ti–6 wt% Al. The package written in Turbo Basic is versatile and can be run to print out maps, using the related stored data files. In modelling the maps, the rate equations governing different deformation mechanisms were employed to find the dominant mechanisms and strain rate contours. In particular, the map for Ti–6 wt% Al was generated and it was found that the power law creep dominated over a wider range of stresses and temperatures than that of pure titanium. It is concluded that the strengthening effect of aluminium has shifted the iso-strain rate contours to higher stresses and temperatures.

1. Introduction

Plastic deformation of engineering alloys, which occurs by a number of alternative mechanisms, is one of the most important design considerations. Deformation-mechanism mapping is a special way of summarizing information about the range of dominance of each of the mechanisms of plasticity, and the rates of flow they produce. This idea was first suggested by Weertman [1, 2] and then developed to the present form by Ashby [3].

The maps are diagrams with axes of normalized shear stress σ_s/μ and temperature T/T_m (where μ is the shear modulus and T_m the melting temperature). They are divided into fields which show the regions of stress and temperature over which each of the deformation mechanisms is dominant. Superimposed on the fields are contours of constant strain rate which show the net strain rate due to the given stress and temperature. The maps display the relationship between the three variables of stress σ_s, temperature T and strain rate $\dot{\gamma}$. If any pair of these variables are specified the maps can be used to determine the third.

The purpose of the present work was twofold. First, to develop simplified computer programs to plot the deformation-mechanism maps for metals and substitutional solid solutions which can be run very simply on microcomputers; and second, to use the package for construction of the map for the Ti–6 wt % Al alloy. Currently the research is continued to further develop the program to construct the maps for more complicated alloys and in particular for Ti–6Al–4V.

2. Calculation procedures

The maps are constructed using two separate computer programs written in BASIC named DEFOR and GRAPH which can be used on microcomputers. DEFOR does all the computations. In the present form these programs can be used to construct the deformation-mechanism maps for all types of metals and solid-solution alloys. The maps can be plotted for all grain sizes, considering the possible allotropic transformations.

In modelling the maps the rate equations governing different deformation mechanisms [4] have been employed to find the dominant mechanisms and strain-rate contours. These deformation mechanisms are dislocation glide (controlled by obstacles and by Peierls resistance), dislocation creep controlled by lattice diffusion and dislocation core diffusion, diffusional creep controlled by bulk diffusion (Nabbarro–Herring creep) and by boundary diffusion (Coble creep), and Harper–Dorn creep.

The rate equations relate the shear strain-rate to shear stress and absolute temperature for each deformation mechanism. The boundary between two successive dominant mechanisms is the locus of all points of stress and temperature at which the dominant mechanism changes. The strain-rate contours are found by calculating the net shear strain-rate value $\dot{\gamma}_{net}$, as follows:

$$\dot{\gamma}_{plas} = \text{least of } \dot{\gamma}_1 \text{ and } \dot{\gamma}_2 \quad (1)$$

$$\dot{\gamma}_6 = \text{greatest of } \dot{\gamma}_{NH} \text{ and } \dot{\gamma}_{HD} \quad (2)$$

$$\dot{\gamma}_{net} = \text{greatest of } [\dot{\gamma}_{plas} \text{ and } (\dot{\gamma}_3 + \dot{\gamma}_4)] + \dot{\gamma}_5 + \dot{\gamma}_6 \quad (3)$$

where $\dot{\gamma}_1$ and $\dot{\gamma}_2$ are the strain rates due to dislocation glide controlled by obstacles and by Peierls resistance, respectively; $\dot{\gamma}_{NH}$ and $\dot{\gamma}_{HD}$ are the strain rates due to the Nabbarro–Herring and Harper–Dorn creep, respectively; $\dot{\gamma}_3$ and $\dot{\gamma}_4$ are the strain-rate values due to dislocation creep controlled by lattice diffusion and dislocation core diffusion, respectively; and finally $\dot{\gamma}_5$ is the strain rate due to Coble creep. For those metals and alloys for which Harper–Dorn creep has not

0022–2461/91 $03.00 + .12

been reported experimentally, upon the user's wish, DEFOR is able to ignore this mechanism. Then Relation 2 will not be executed and $\dot{\gamma}_6$ will be simply $\dot{\gamma}_{NH}$. On the other hand, when there is no field of dominance of Harper–Dorn creep, this in turn will suggest the range of the values of the variable parameters of stress, temperature and grain size for experimental work to find the actual field of dominance of Harper–Dorn creep.

For M-type and dilute A-type binary solid-solution alloys, knowing the diffusion data for the solute and the matrix, the program is capable of plotting the map for the alloy, while in calculating creep strain rates it distinguishes between M-type and A-type alloys [5]. When there exist enough diffusion data for the alloy and in the case of high-concentration A-type alloys, data for the alloy are used directly to plot the map.

In construction of the map for Ti–6 wt % Al (Fig. 1) some of the required data were gathered from the literature, while others were estimated using the data for materials in the same class of mechanical behaviour. These data are shown in Table I. Diffusion data for titanium and aluminium [4] were used for calculating creep strain rates. This alloy is considered to be an M-type alloy [6]. It is to be noted that there exist a few data for the β phase of Ti–6 wt % Al, a prototype of α-titanium alloys. For completing the visual form of the map we have used the data for β-Ti [6] in the β phase of the alloy.

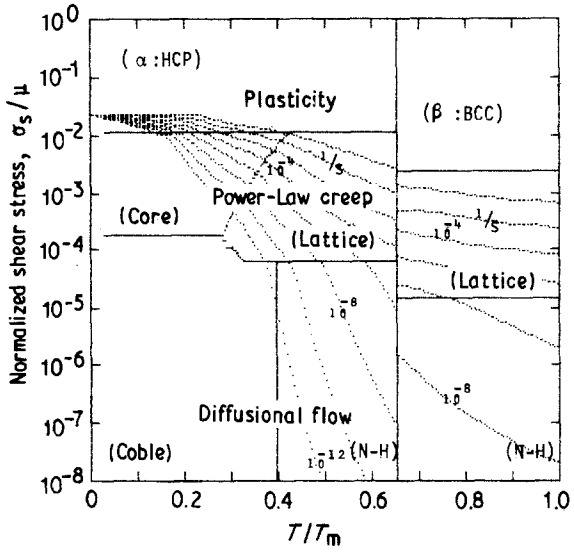

Figure 1 Deformation mechanism map for Ti–6 wt % Al with a grain size of 100 μm.

TABLE I Material data for α phase of Ti–6 wt % Al

Material property	Data	Ref. or note
Crystallographic and thermal data		
Atomic volume, Ω (m^3)	1.76×10^{-29}	a
Burgers vector, b (m)	2.89×10^{-10}	a
Melting temperature, T_m (K)	1918	[13]
Transition temperature, T_t (K)	1253	[13]
Modulus		
Shear modulus at 300 K, μ_0 ($N m^{-2}$)	4.7×10^{10}	[14]
Temperature dependence of μ, $d\mu/dt$ ($N m^{-2} K^{-1}$)	-2.8×10^7	b
Nabbarro–Herring creep		
Pre-exponential, D_{0v} ($m^2 sec^{-1}$)	1.3×10	a
Activation energy, Q_v ($J mol^{-1}$)	2.47×10^5 to 2.64×10^5	[15]
Coble creep		
Pre-exponential, δD_{0b} ($m^2 sec^{-1}$)	3.6×10^{-16}	a
Activation energy, Q_b ($J mol^{-1}$)	1.23×10^5 to 1.32×10^5	c
Power-law creep		
Exponent, n	4.3	b
Dorn constant, A	1×10^3	a
Power-law breakdown, σ_s/μ_0	3.5×10^{-3}	a
Core diffusion		
Pre-exponential, $a_0 D_{0c}$ ($m^4 sec^{-1}$)	7.8×10^{-26}	a
Activation energy, Q_c ($J mol^{-1}$)	1.23×10^5 to 1.32×10^5	b
Lattice diffusion		
Pre-exponential, D_{0cr} ($m^2 sec^{-1}$)	1.3×10^2	d
Activation energy, Q_{cr} ($J mol^{-1}$)	2.47×10^5 to 2.64×10^5	d
Obstacle-controlled glide		
0 K flow stress, τ_0 ($N m^{-2}$)	1.26×10^9	b
Pre-exponential γ_0 (sec^{-1})	1×10^6	[16]
Activation energy, ΔF (N m)	2.68×10^{-19}	e

[a] Assumed to be the same as titanium.
[b] Inferred from data for alloys in the same class of mechanical behaviour [6].
[c] $Q_b = \frac{1}{2} Q_v$ [17].
[d] $D_{cr} = D_v$ for the alloy, then $D_{0cr} = D_{0v}$ and $Q_{cr} = Q_v$.
[e] $\Delta F = 0.2 \mu b^3$ [8].

3. Results and discussion

The programs are versatile and can be run to print out the maps for pure metals and solid-solution alloys with different grain sizes. We have reconstructed the maps for pure titanium (Fig. 2), aluminium and nickel [6] which were previously presented by Ashby and co-workers [4, 7, 8]. The map for pure titanium with a grain size of 220 μm has also been plotted to show the range of dominance of Harper–Dorn creep (Fig. 3) which is experimentally reported by Malakondaiah and Rao [9–11] at large grain sizes. In calculating the strain-rate values for Harper–Dorn creep the value of the dislocation density ρ for titanium was assumed to be 3×10^8 m^{-2} in order to match the experimental data, which give an approximate minimum grain size of 200 μm for the occurrence of this deformation process at high temperatures and low stresses [6, 11].

In this work we have considered those deformation mechanisms which have practical importance. Deformation processes such as phonon or electron drag and adiabatic shear are not included, since these concepts have not yet been practically developed.

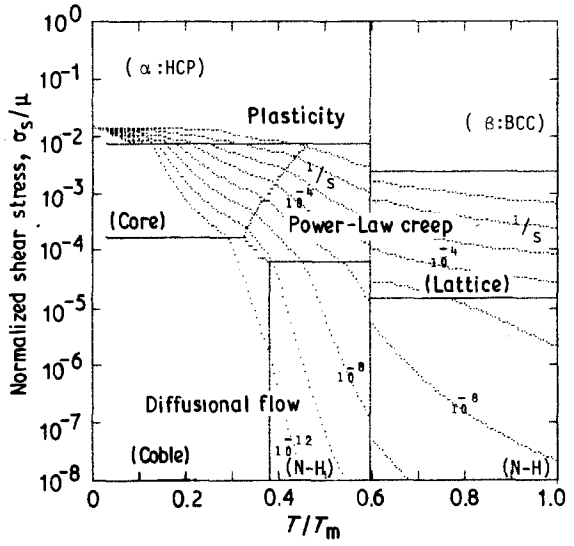

Figure 2 Deformation mechanism map for titanium with a grain size of 100 μm.

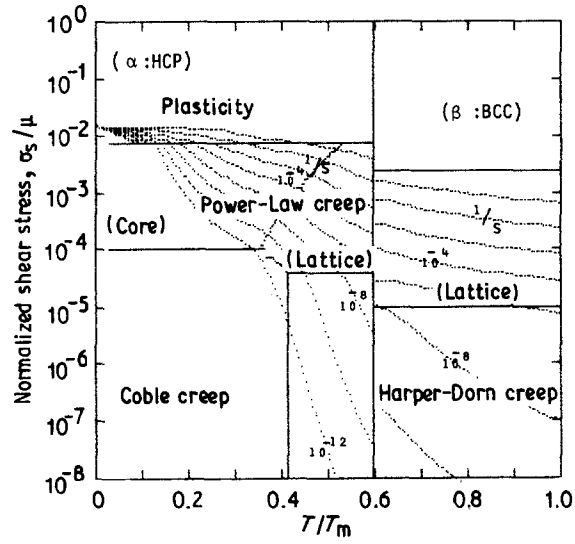

Figure 3 Deformation mechanism map for titanium with a grain size of 220 μm.

The method that we have chosen for the superposition of the rate equations (Relations 1 to 3) differs from that of Frost and Ashby [4] in considering the Harper–Dorn creep as an alternative for Nabbarro–Herring creep. They have assumed that the Harper–Dorn creep mechanism replaces diffusional flow (Nabbarro–Herring + Coble creep) at large grain sizes. Our assumptions have been found to be in better agreement with the experimental results reported by other researchers [6, 9–12]. At a critical grain size the two mechanisms of Harper–Dorn and Nabbarro–Herring creep may coexist [12] and this is considered in construction of the maps [6].

The strengthening of aluminium as an alloying element for titanium has been studied by comparing the maps for Ti–6 wt % Al and pure titanium (Figs 1 and 2). The results are summarized as follows:

1. The yield stress at low temperatures is increased.
2. The dislocation glide region is shifted to higher stresses.
3. The range of dominance of dislocation creep controlled by lattice diffusion is expanded and that of dislocation creep controlled by core diffusion is reduced, which shows the effect of solute atoms as barriers to diffusion through the dislocation core.
4. The region dominated by Nabbarro–Herring creep is enlarged and that of Coble creep reduced, showing the effect of solute atoms as barriers to diffusion through the grain boundaries.
5. The iso-strain rate contours have been shifted to higher stresses and temperatures.

Acknowledgement

The authors wish to express their gratitude for the financial support of this research to the Shiraz University Research Council under grant No. 67-EN-475-245.

References

1. J. WEERTMAN and J. R. WEERTMAN, in "Physical Metallurgy", edited by R. W. Cahn (North-Holland, Amsterdam, 1965) p. 793.
2. J. WEERTMAN, *Trans. Amer. Soc. Metals* **61** (1968) 681.
3. M. F. ASHBY, *Acta Metall.* **20** (1972) 887.
4. H. J. FROST and M. F. ASHBY, "Deformation-Mechanism Maps" (Pergamon, Oxford, New York, Toronto, Sydney, Paris, Frankfurt, 1982).
5. T. G. LANGDON, in Proceedings of 3rd International Conference on the Strength of Metals and Alloys, Melbourne, Australia, 16–20 August 1982, edited by R. G. Gifkines (Pergamon, Oxford, New York, 1983) p. 1105.
6. S. ESMAEILI, MS thesis, Shiraz University (1988).
7. P. M. SARGENT and M. F. ASHBY, *Scripta Metall.* **16** (1982) 1415.
8. M. F. ASHBY, in Proceedings of 3rd International Conference on the Strength of Metals and Alloys, Cambridge, UK, 20–25 August 1973, Vol. 2, edited by R. G. Gifkines (Inst. Met. Lond. Monogr. Rep. Ser. n 36, 1973) p. 8.
9. G. MALAKONDAIAH and P. RAMA RAO, in "Mechanical Behavior of Materials-IV", edited by J. Carlsson and N. G. Ohlson (Pergamon, Oxford, New York, 1984) p. 337.
10. *Idem., Scripta Metall.* **13** (1979) 1187.

11. *Idem., Acta Metall.* **29** (1981) 1263.
12. T. G. LANGDON and F. A. MOHAMED, *J. Mater. Sci.* **13** (1978) 1282.
13. "Metals Handbook", 8th Edn, Vol. 8 (ASM, Metals Park, Ohio, 1973) p. 264.
14. S. G. FEDOTOV, in "Titanium and Its Alloys", edited by I. I. Kornilov (IPST, Jerusalem, 1966) p. 199.
15. R. D. FRENCH, in "Titanium Science and Technology", Vol. 4, edited by R. I. Jaffee and H. M. Burte (Plenum, New York, London, 1973) p. 2195.
16. H. J. FROST and M. F. ASHBY, in "Rate Processes in Plastic Deformation of Materials", edited by J. C. M. Li and A. K. Mukherjee (ASM, Materials/Metal Working Technology Series, 1975) p. 70.
17. S. C. MISRO and A. K. MUKHERJEE, in "Rate Processes in Plastic Deformation of Materials", edited by J. C. M. Li and A. K. Mukherjee (ASM, Materials/Metal Working Technology Series, 1975) p. 434.

Received 5 December 1989
and accepted 13 August 1990